Fiber Optical Micro-detectors for Oxygen Sensing in Power Plants

Quarterly Technical Report
Reporting Period:
January 1, 2005 to March 31, 2005

Gregory L. Baker*, Ruby N. Ghosh[+], D.J. Osborn III*, Po Zhang[+]

April 2005

DOE Award Number: DE-FC26-02NT41582

*536 Chemistry Building, Department of Chemistry
[+]2170 BPS, Center for Sensor Materials and Dept. of Physics
Michigan State University

DISCLAIMER

ABSTRACT

A reflection mode fiber optic oxygen sensor that can operate at high temperatures for power plant applications is being developed. The sensor is based on the $^3O_2$ quenching of the red emission from hexanuclear molybdenum chloride clusters. One of the critical materials issues is to demonstrate that the luminescent cluster immobilized in the sol-gel porous support can withstand high temperature. At the same time the sol-gel matrix must have a high permeability to oxygen. Using a potassium salt of the molybdenum clusters, $K_2Mo_6Cl_{14}$, we have established the conditions necessary for deposition of optical quality sol-gel films. From spectroscopic measurements of the film we have shown that the cluster luminescence is stable following heat cycling of 54 hours at 200°C. Quenching of a factor of 1.5X between pure nitrogen and 21% oxygen was observed from *in-situ* measurements of films heated directly at 200°C. An automated system for characterizing fiber optic oxygen sensors up to 220 °C with a temporal resolution better than 10 s is under construction. We estimate a signal of 6×10^8 photons/s after complete quenching in 21% oxygen. These are promising results for a high temperature fiber optical oxygen sensor based on molybdenum chloride clusters.

TABLE OF CONTENTS

INTRODUCTION

Maximizing the efficiency of the combustion process requires real-time control of the correct fuel/oxygen ratio. This requires the ability to sense oxygen levels over a broad range of concentrations with fast response times. Mussell, Newsham, and Ruud previously reported preliminary studies of the synthesis and optical properties of Mo_6Cl_{12}-based clusters relevant to this project [1-4]. Mussell described the synthesis of the molybdenum clusters, and Newsham gives a good account of the properties of neutral Mo_6Cl_{12} clusters and their salts, in both solution and a sol gel matrix. Newsham's data indicate that the photophysical properties of the clusters are maintained in sol gel matrices. To prepare a fiber optic sensor based on Mo_6Cl_{12}, Ruud dispersed Mo_6Cl_{12} in poly[1-trimethylsilyl-1-propyne] (PTMSP), and used a dipping technique to immobilize the composite at the cleaved end of a silica optical fiber. Ghosh and co-workers [5] demonstrated a fast room temperature fiber optic sensor based on oxygen quenching of the luminescence from the PTMSP/Mo_6Cl_{12} composites. While the PTMSP support is adequate for room temperature applications, is unable to withstand the high temperatures associated with combustion in a power plant. To improve the sensor's high temperature performance, we are replacing PTMSP with a thermally stable sol gel matrix that should be able to withstand the higher temperature requirements of the power plant combustion process. The idea of using a sol gel as the support matrix for high temperature oxygen sensor application is not new. Remillard and coworkers have shown that a sol gel supported copper based oxygen sensor can be used in a combustion process [6]. With these facts in hand, we anticipate promising results from our design.

EXECUTIVE SUMMARY

A requirement of optical sensors based on luminescence quenching is that the lumophore have a strong luminescence that is efficiently quenched by oxygen, and that oxygen has ready access to the lumophore. For a high temperature sensor, these characteristics must hold over the entire temperature range of interest.

A series of long-term aging experiments were carried out on samples that were heated to 200 °C for various times. The results show that the luminescence intensity as measured in nitrogen at room temperature remains constant despite greater than 50 hours of cumulative annealing at 200 °C. Note that these results fulfill our milestone for 1/30/05 – 3/31/05 "Will investigate the thermal stability of alkali metal salt derivatives of Mo_6Cl_{12}". The quenching ratio, as defined by the luminescence intensity in nitrogen divided by the intensity in air, decreased with annealing at 200 °C. Real-time measurements of the luminescence intensity as a function of temperature show that the luminescence intensity decreases reversibly with increasing temperature (up to 210 °C) with a quenching ratio <2. A synthetic challenge is to increase the quenching ratio to four or better. Adding nanoparticulate fumed silica to the sol-gel preparations initially improved the quenching ratio but did not improve the long-term stability at 200 °C.

We devised and verified a routine synthesis of $K_2Mo_6Cl_{14}$. Characterization of two separate lots prepared by this method using thermogravimetric analysis, UV/vis spectroscopy, and luminescence spectroscopy showed that the lots were identical to an earlier sample used for most of the work in this project. This synthetic scheme is capable of generating multi-gram quantities of the inorganic lumophore as needed. We improved the quality of planar substrates coated with $K_2Mo_6Cl_{14}$ in sol-gel matrices by devising a dip coater capable of coating slides at a slow and constant rate. We also investigated the use of spray coating for coating planar substrates and the tips of high-temperature optical fibers. A comparison of the resulting film thicknesses with the optical characteristics of high-temperature fibers suggest that the sol-gel films need to be substantially thicker than can be easily obtained by either method. Our proposed solution is to modify the sol-gel solution and spray coat the tips of fibers with a slurry of cured $K_2Mo_6Cl_{14}$/sol-gel nano particles in a sol-gel solution.

An automated system for characterizing high-temperature optical fibers coated with $K_2Mo_6Cl_{14}$/sol-gel films at elevated temperatures has been designed to test the performance of sensors at elevated temperatures. Time resolved measurements, $t < 10$ s, will be possible using the system. After consulting with several manufacturers we have purchased two different UV transparent optical fibers from Fiber Guide and Ceramoptec, rated for continuous operation at 200 and 400 °C respectively. We calculate that for the Ceramoptec fiber a sensor signal of 6×10^8 photons/s after complete quenching in 21% oxygen. The typical detector dark counts are ~1000, so we have more than sufficient signal to noise for a $K_2Mo_6Cl_{14}$ based high temperature fiber sensor.

A provisional patent application covering parts of this work in was filed in January 2005, #60/648,367 “Sol-gel encapsulated metal halide cluster for optical fiber sensing of oxygen”.

EXPERIMENTAL

Materials.

All glassware was oven-dried prior to use. Acetonitrile (Spectrum Chemical Company, HPLC grade) was dried over CaH_2 and distilled prior to use. Tetraethyl orthosilicate (TEOS) (Aldrich, 98%) and hydrochloric acid (CCI, electronics grade) were used as received. Corning 7980 quartz microscope slides (3" × 1" × 1 mm) were obtained from Technical Glass Products and cut into 1.25 cm × 2.45 cm pieces. Slides were handled with gloves and tweezers in order to minimize surface contamination.

Preparation of the Mo_6Cl_{12} hydrochloride salt.

$MoCl_2$ from City Chemical (lots 40C65 and 40M21) was received as a yellowish-green powder with small dark-blue specks and was purified by conversion to the Mo_6Cl_{12} hydrochloride salt. A representative procedure is described. $MoCl_2$ (2g) and 800 mL of 6M HCl were added to a 1 L Erlenmeyer flask and stirred with a Teflon coated magnetic stir bar. The solution was heated to the boiling point for several hours and the resulting bright-yellow solution was then filtered through medium-fast filter paper to remove insoluble white and metallic particles. The filtered solution was heated on a hot plate and the volume reduced to 200 mL. The hot plate was turned off and the solution was left on the hot plate to slowly cool to room temperature. A small amount of seed crystals were added and yellow crystals formed overnight. After cooling the solution in an ice bath for 5 hours, the resulting yellow crystals of the hydrochloride salt were collected by gravity filtration through Whatman medium-fast filter paper. The crystals were then placed onto several pieces of filter paper and allowed to dry under ambient conditions for two days. Yield: 586 mg. A second crop of crystals was obtained by heating to concentrate the mother liquor to 100 mL, filtration, and a further reduction in volume to 50 mL. Cooling, seeding the solution as described above, and storing the solution in a freezer overnight yielded long yellow needles. Drying the needles on filter paper yielded 256 mg of the Mo_6Cl_{12} hydrochloride salt. The products were characterized using x-ray powder diffraction, UV-vis spectroscopy, fluorescence spectroscopy, and energy dispersive x-ray spectroscopy.

Standardized synthesis of the potassium salt of Mo_6Cl_{12}. ($K_2Mo_6Cl_{14}\cdot 2H_2O$)

With heating, dry Mo_6Cl_{12} (1.0546 g, 1.055 mmol) was dissolved in 500 mL of 6M HCl in a 1 L Erlenmeyer flask. The hot solution was filtered (Whatman, medium speed) to and then the volume was reduced to 250 mL by boiling. A saturated solution of KCl in 6M HCl (200 mL) was added to hot solution, and then the volume was further reduced to 150 mL by boiling. After cooling slowly to room temperature and an addition 24h at room temperature, yellow needle-like crystals of $K_2Mo_6Cl_{14}$ were collected by filtration. Drying under ambient conditions for three days yielded 1.0132 g of $K_2Mo_6Cl_{14}\bullet H_2O$. The product was analyzed by TGA, UV-vis, fluorescence, and XPD.

Film Deposition.

A typical stock sol-gel solution for the coating process was prepared as described below. TEOS (100 mL, 0.477 mol) and acetonitrile (70.3 mL) were added to a 500 mL Erlenmeyer flask. With stirring, water (32.3 mL, adjusted to pH=1 with HCl) was added

and the solution was stirred for 1 hour at room temperature. The stir bar was removed from the flask and the solution was heated in an oil bath at 70 ºC for 2.5 hours. The solution was then transferred to a 500 mL glass bottle, capped, and aged at room temperature until use. For the 29 series of samples, 25.5 mg of $K_2Mo_6Cl_{14}\cdot 2H_2O$ was added to the vial approximately three days before dipping the slides, and the solution was stirred for three days to ensure complete dissolution of the complex. For the 30 series of samples, the process was identical except 62.2 mg of $K_2Mo_6Cl_{14}\cdot 2H_2O$ was added to 15 mL of stock solution.

Dip coating at controlled dipping rates. Just prior to use, the slides were removed from distilled water and dried by under a stream of nitrogen gas. For some slides, one surface was masked using a piece of Scotch Magic™ tape to limit the sol-gel coating to one side of the substrate. A simple dip coater was built to better control the uniformity of coated slides, especially at low dipping rates (~1 mm/sec). Slides were clamped in the dip coater, dipped with no hold time and placed directly into a 20 mL scintillation vial. The vial was capped and stored on its side to minimize flow of the solution. By varying the dip rate and assessing film quality, we determined that a dip rate of 1 to 1.6 mm/sec gave the best quality films. Since vial containing the sol-gel solution was left uncapped between coats solvent evaporation led to an increase in viscosity which limited the number of slides that could be dipped from a given solution. Replenishing the ethanol while dipping greatly increased the lifetime of the sol-gel solution. The films were thermally cured in air at 200 ºC for 30 minutes

Spray coating.
Following the procedure described by Remillard et al., [6] viscous sol-gel solutions containing $K_2Mo_6Cl_{14}$ were applied to substrates using a Paasche double action airbrush. Fibers were supported in the barrel of a hypodermic syringe ~4 cm from the tip of the spray coater. The fiber was coated in 1 second bursts aimed directly at the tip with 15 seconds of dry time in between each burst. The pressure of gas supplied to the airbrush was set at 10 psi, and the spray burst size was varied to determine the optimal spray conditions. Planar substrates were coated similarly.

Optical microscopy of thin films.
Polarized optical microscopy images were acquired using a Nikon Optiphot2-Pol equipped with a Sony Hyper HAD CCD-IRIS/RGB color video camera (model DXC-151A). The camera was connected to a PC using a Sony camera adapter (model CMA-D2). The images were viewed using a Sony Trinitron color video monitor. Images were taken using Hauppage computer works Win/TV software (version 2.4.17052).

Absorption spectroscopy.
Samples were prepared by weighing 2 - 3 mg of Mo_6Cl_{12} in a small sample vial. The compound was then dissolved in a small amount of dry acetonitrile and transferred to a 10 mL volumetric flask. The volumetric flask was filled to the mark, stoppered, and shaken to insure a homogenous solution. Typical concentrations were 1.7×10^{-4} M. Absorption spectra were measured using a Perkin-Elmer Lambda 40 series double beam UV/vis spectrometer. Data analysis was performed using the UV Win lab (version 2.80.03) software package supplied with the instrument and plotted using Microsoft

Excel. Solutions were placed into a 1 cm pathlength quartz cuvette with a separate cell containing only solvent as a reference.

Fluorescence measurements

The fluorescence measurements were performed using a Fluorolog-3 instrument from Instruments S.A., Inc. The system includes a single Czerny-Turner excitation spectrometer with a 1200g/mm ruled grating blazed at 330nm and a single Czerny-Turner emission spectrometer with a 1200g/mm holographic grating blazed at 630 nm. The excitation optics consists of a 450W ozone free Xe lamp, followed by a 270-380 nm bandpass filter (Oriel 1124). A Si photodiode is used to continuously monitor the lamp signal. The detection optics consists of 603.2 nm long wave pass filter (CVI) followed by a multi-alkali photo multiplier tube (Hamamatsu R928) with photon counting electronics. Data processing was performed using the Datamax (version 2.2) software package supplied with the instrument. Spectra were obtained by exciting at 313 nm and scanning the emission monochromator from 550 to 850 nm.

Measurements of cluster fluorescence in solution were performed by placing the solution in a quartz cuvette sealed with an airtight septum. Spectra were measured in laboratory air and high purity nitrogen (AGA, Inc, 99.999%). Prior to obtaining spectra, all gases were bubbled through the solution for 10 to 15 minutes at a rate of ~10 mL / min. via a glass pipette inserted through the septum. For the measurements of the potassium salts in HCl a glass pipette was used to bubble oxygen into the solution.

The measurements of the $K_2Mo_6Cl_{14}$ emission from Mo-cluster / sol-gel composite films were made in the quartz cuvette sealed with an airtight septum. Nitrogen gas with purity 99.999% was used to obtain the luminescence spectra in a non-oxygen environment. The oxygen measurements (21% oxygen in nitrogen) were performed using 99.999% purity gas. The nitrogen and oxygen were injected bias a needle passing through the septum and allowing the gas in the cuvette to equilibrate for 10 min. An external gas flow switch was designed and built to conveniently change the gas environment without needing to touch the spectrometer compartment. This switch allows us to be completely certain that the sample does not move during repeated gas exchange.

The *in-situ* measurements of the Mo_6Cl_{12} emission from Mo-cluster / sol-gel composite films, as a function of temperature were made in the same quartz cuvette described above. A platinum microheater (part 32 208 172 from Heraeus Sensor Technology) was attached with a thermally conducting epoxy resin (Ther-O-Bond/1500 hardener) to the backside of the quartz slide. The epoxy is allowed to cure for at least four hours in air at room temperature. Electrical connection to the Pt heater was made by microwelding 5 mill thick Cu wire to the 5 mill thick legs of the Pt microheater. The electrical leads were then threaded through the septum. The microheater was powered with a regulated voltage supply. We determined the heater temperature by monitoring the heater resistance, and using the resistance versus temperature curves for a standard 100 ohm Pt thermometer. The thermal impedance of the quartz slide was independently determined by gluing a Pt thermometer to the front of a quartz slide, and monitoring the temperature of the front side of the slide in the quartz cuvette under the same gas flow conditions used during spectroscopy. Thus, by monitoring the backside heater resistance we know the temperature of the front side of the slide to ±5 °C.

Thermal Analysis

Isothermal aging of $K_2Mo_6Cl_{14}$ was run in air using a Perkin Elmer TGA-7 system, which consists of a computer, TGA-7 low temperature furnace and balance module, and a TAC7/DX controller. The flow-rate of balance and sample gas was 45 and 40 mL/min respectively. The pan, stirrup and hanger wire were made of platinum metal that was connected to a gold balance wire using a quartz hook. Samples were first equilibrated at 115 °C for 1 hour to remove residual water, and then heated to 280 °C at a rate of 10° per minute.

RESULTS AND DISCUSSION

Materials synthesis and characterization goals in the current reporting period include the development of a standardized method for preparing $K_2Mo_6Cl_{14}$, routine deposition of homogeneous thin films on quartz substrates for optical characterization, and immobilization of clusters at the tip of a high-temperature optical fibers. The optical propoerties of specific samples are described in this report. The synthetic protocol used to prepare the slides is shown in Figure 1.

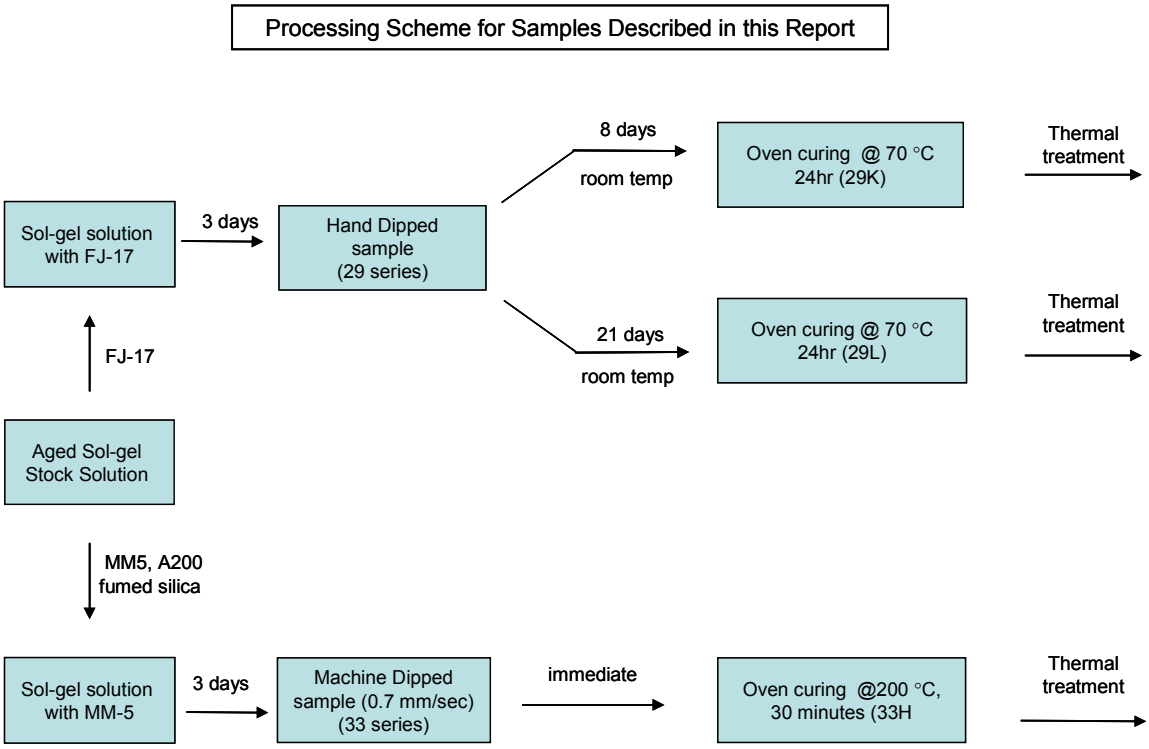

Figure 1. Processing scheme used to preare samples described in this report. Films 29K, 29L and 33H were studied via spectroscopy.

Standardized syntheses of $K_2Mo_6Cl_{14}$.

In the previous reporting period we showed that $K_2Mo_6Cl_{14}$, the potassium salt of Mo_6Cl_{12}, has superior thermal stability compared to Mo_6Cl_{12}. One of the simplest and most effective methods for characterizing new samples of $K_2Mo_6Cl_{14}$ is to carry out isothermal aging experiments. The potassium salt shows at most a few percent weight loss during four hours of isothermal aging at 280 °C in air. In contrast, samples contaminated with Mo_6Cl_{12} degrade significantly and lose substantial weight early in the isothermal aging experiment. We prepared two large scale batches of the potassium salt, MM-7 and MM-8, and measured their isothermal aging characteristics. As shown in **Figure 2,** their thermal degradation profiles are nearly identical to FJ-17, an earlier preparation of $K_2Mo_6Cl_{14}$ that we widely used as the lumohore in much of our data reported to date. The profile of another lot (MM-5) prepared at approximately the same time as FJ-17 shows a significant weight loss early in the run, and we conclude from its

similarities to the weight loss profile of Mo_6Cl_{12} that MM-5 is contaminated by the less stable Mo_6Cl_{12}.

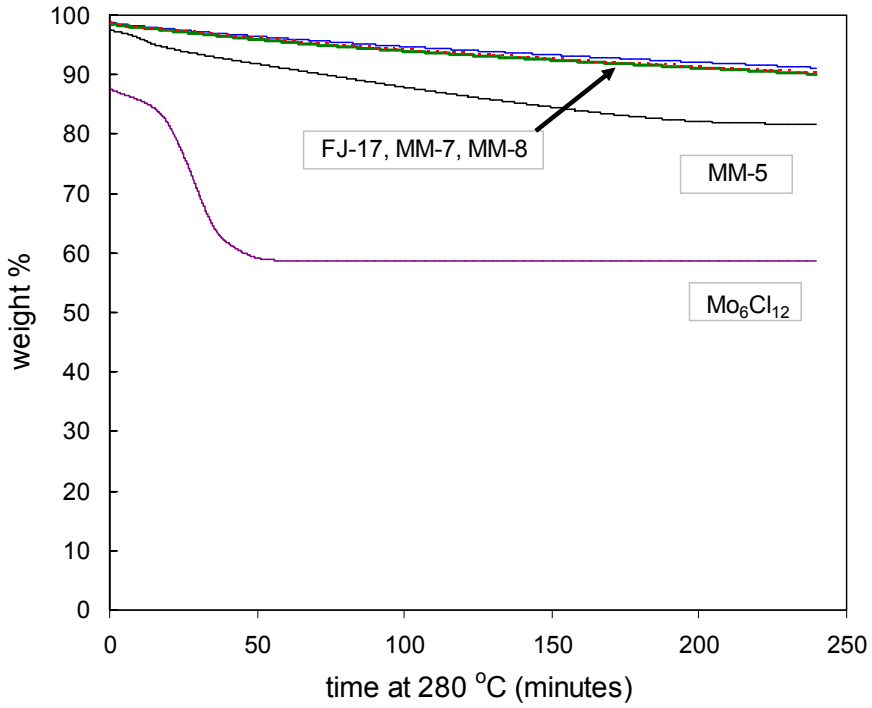

Figure 2: Isothermal aging tests of four preparations of $K_2Mo_6Cl_{14}$ (FJ-17, MM-5, MM-7, and MM-8 at 280 °C in air, showing the consistent thermal profiles of recently prepared batches of $K_2Mo_6Cl_{14}$ The corresponding data for Mo_6Cl_{14}•2HCl are shown for comparison

While characterizing the weight loss profile of a candidate salt is a rapid assay for the purity of the salt, a more rigorous test is measurement of the optical properties of the lumophore. Solutions of MM-7, MM-8, and FJ-17 were prepared in acetonitrile and their luminescent properties were measured. Data measured at room temperature shown in **Figure 3**, demonstrate that both the line shape and luminescence intensity of for all three samples are nearly identical and are consistent with the notion that the lumophores in FJ-17, MM-7 and MM-8 are identical. Samples of the same salts were then heated to 200 °C for four hours, cooled to room temperature, and again solutions of the salts in acetonitrile were prepared and their luminescent properties were measured. The results again are consistent with the conclusion from the isothermal aging experiments, that the clusters from all three batches are identical. Note that the as expected the emission intensity scales linearly with cluster concentration.

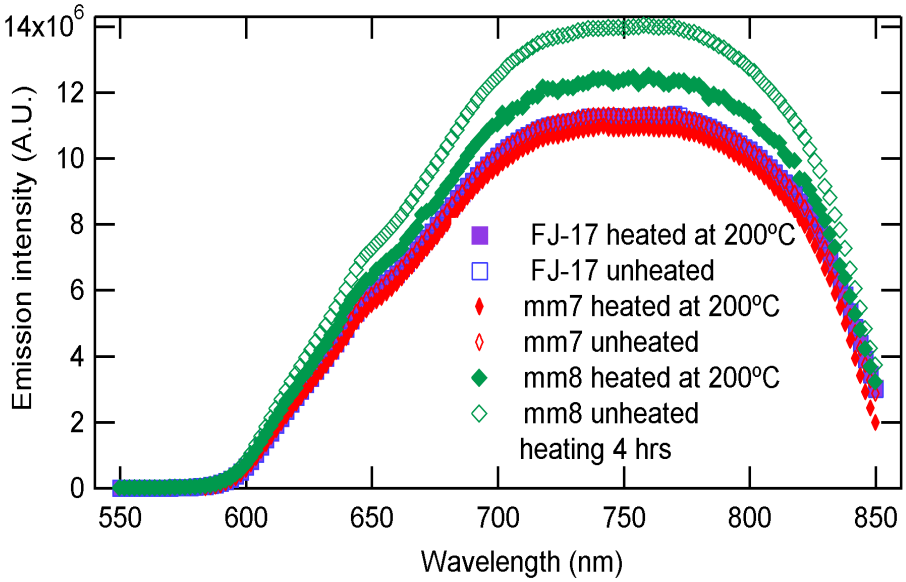

Figure 3: A comparison of the emission spectra from three different preparations of $K_2Mo_6Cl_{14}$, FJ-17, MM-7, and MM-8. Data are shown for as-prepared samples, as well as samples that have been heated to 200° for 4 hours, illustrating that both lineshape and intensity are conserved. Solution concentrations: **MM-8**: 0.118 mM ±1.4%_and 0.115 mM ±1.4% after heating; **MM-7**: 0.0959 mM_±1.4%, and **FJ-17:** 0.087 mM_±1.4%. Within the error bars of the measurement the emission intensity scales with concentration.

While the data presented above emphasize the similarity of the three different batches of potassium salt, UV/vis data suggest that there may be a silent impurity present in all three samples. UV/vis spectra were taken of the three salts as solutions in acetonitrile. As shown in **Figure 4** the spectra have similar but not identical line shapes. While the low energy side of the absorption envelope (>350 nm) for all three salts appear to be identical, the spectra of the three salts differ at shorter wavelengths. The data suggest an additional absorbance feature centered at 300 nm for MM-7 and MM-8. Additional experiments on FJ-17 confirms that this feature is present in all three samples, and its intensity is related to the age of the solution. Since the absorption envelope for $\lambda > 350$ nm remains unchanged in intensity and shape as the 300 nm grows in, we speculate that the increase in absorption at 300 nm is due to a nanoparticulate impurity that is not removed by filtration during purification of the salts. When dispersed in acetonitrile, the impurity apparently dissolves to give a soluble Mo complex with an absorption peak at 300 nm. Since the luminescence spectra do not show the same effect, the impurity is apparently non-luminescent and does not interfere with the luminescence quenching of $K_2Mo_6Cl_{14}$. Despite the fact that this impurity appears to be innocuous, we will try to devise method for removing it from the salt.

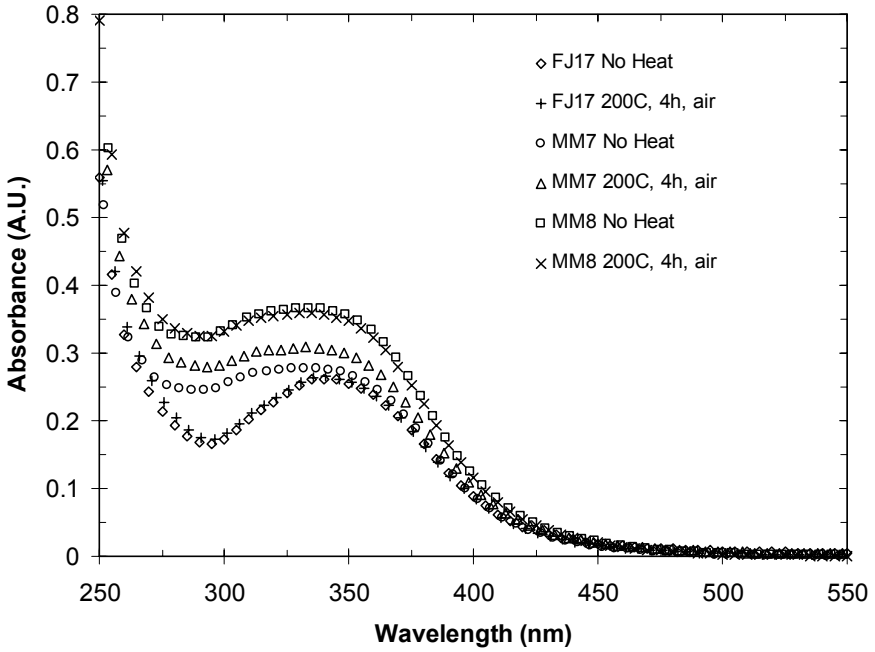

Figure 4: UV/vis spectra from three different preparations of $K_2Mo_6Cl_{14}$, FJ-17, MM-7, and MM-8. Data are shown for as-prepared samples, as well as samples that have been heated to 200 °C for 4 hours. The intensity of the "excess" absorption centered at 300 nm correlates with the age of the solutions. Solution concentrations: **MM-8**: 0.118 mM ±1.4% and 0.115 mM ±1.4% after heating; **MM-7**: 0.0959 mM ±1.4%, and **FJ-17** 0.087 mM ±1.4%.

Deposition of sol-gel matrices containing $K_2Mo_6Cl_{14}$ clusters on planar and fiber substrates.

Coating quartz substrates with $K_2Mo_6Cl_{14}$clusters embedded in sol-gel films is a key prerequisite for studying the temperature dependent photophysics of $K_2Mo_6Cl_{14}$ clusters relevant to oxygen sensing based on luminescence quenching. The film requirements are high optical clarity (absence of cloudiness or substantial cracking), mechanical stability (good adhesion), uniformity in thickness and a sufficient concentration of clusters to support luminescence and quenching measurements over a broad range of temperatures. We recently moved from a hand dipping technique for preparing planar substrates to a mechanized scheme where the rate at which substrates are drawn from sol-gel solutions can be more precisely controlled. Using constant dipping rates resulted in an immediate improvement in film quality as evidenced by smooth films with decreased frequency of cracks and films. The apparatus used for the dipping process shown in **Figure 5**.

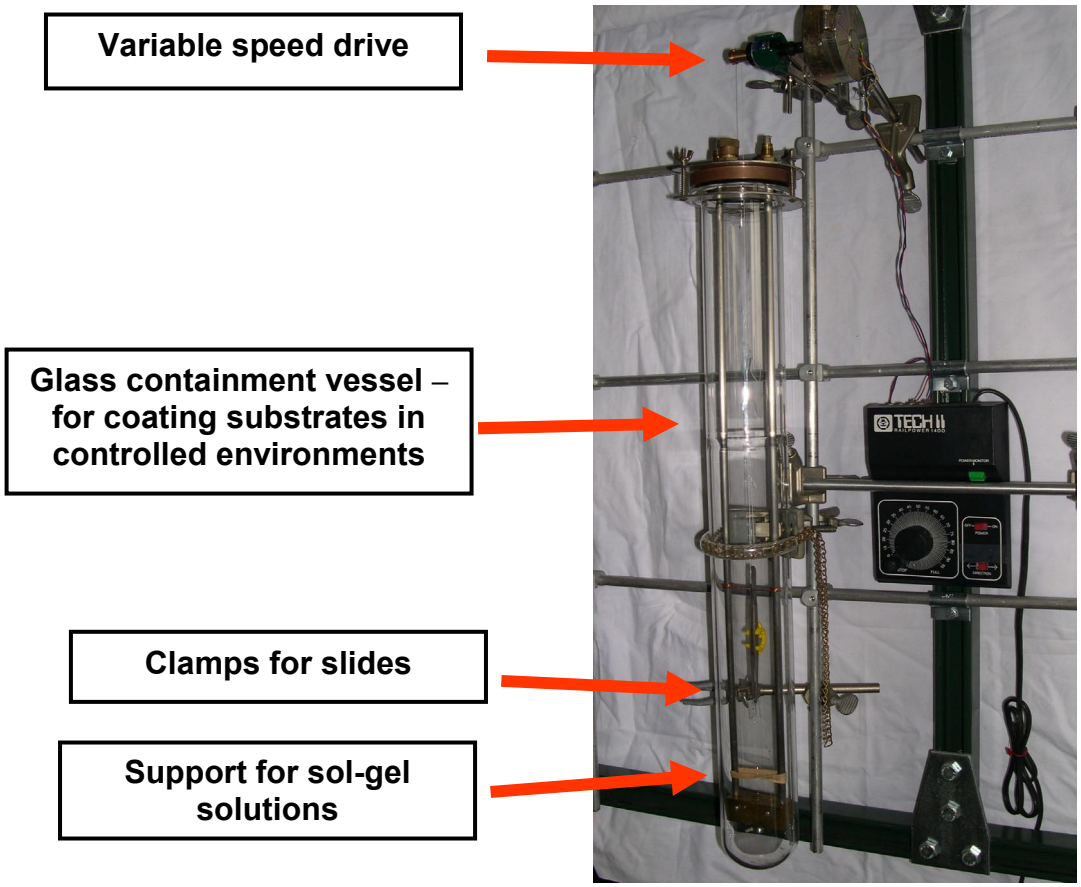

***Figure 5*:** Apparatus used for controlled coating of planar substrates. The overall height is of the apparatus is approximately one meter

A second technique suitable for deposition of films on substrates is spray coating. Advantages of spray coating include the ability to deposit thin films uniformly and

rapidly on surfaces, rapid drying times, and high throughput. A disadvantage of spray coating is that the resulting films generally are quite thin, often on the order of 1 μm. A convenient way of applying films in the laboratory scale is to use the commercial airbrush. Shown in **Figure 6** is a simple rig for spray deposition on planar substrates and at the tips of fibers. The target and the spray apparatus can be enclosed to control the evaporation rate of the solvent. Our experience with coating planar substrates with the sol-gel matrices is that the film clarity and depletion is excellent. Since the films are thin, significant cracking characteristic of thicker films is avoided. These films are suitable for spectroscopic measurements of the clusters embedded in the matrix. However multiple coats need to be deposited to obtain thicker films so that the signal from the lumophores is sufficiently strong for simple optical detection of the luminescence quenching.

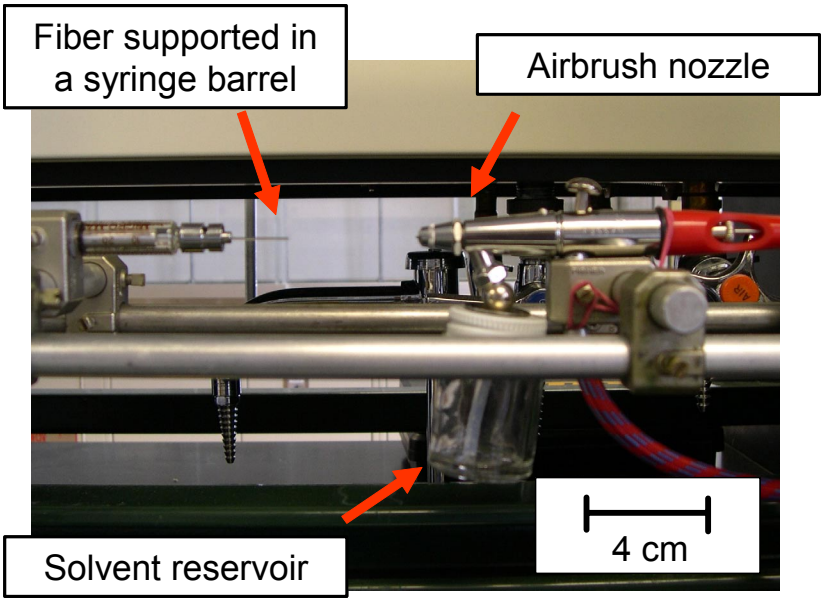

***Figure 6*:** Apparatus used for spray coating of high temperature optical fibers

Deposition of sol-gel films on fibers is more challenging. Our spray coating results to date have been disappointing in that we have been unable to apply multiple coatings to build up thick films and at the same time avoid cracking. A typical spray coating result is shown in the optical micrographs in **Figure 7**. Cracking in the sol-gel film spray coated on the surface of a high-temperature optical fiber is conspicuous. In addition the thinness of the film translates into a low absolute number of clusters available for sensing. Simply increasing the concentration of clusters in the sol-gel solution is limited to the low solubility of clusters in the acetonitrile solvent. Another disadvantage of spray coating with clusters dissolved in a sol-gel solution is that the sol-gel matrix undergoes a large decrease in volume as the sol-gel matrix cures. The large internal stress in such films exacerbates potential cracking problems.

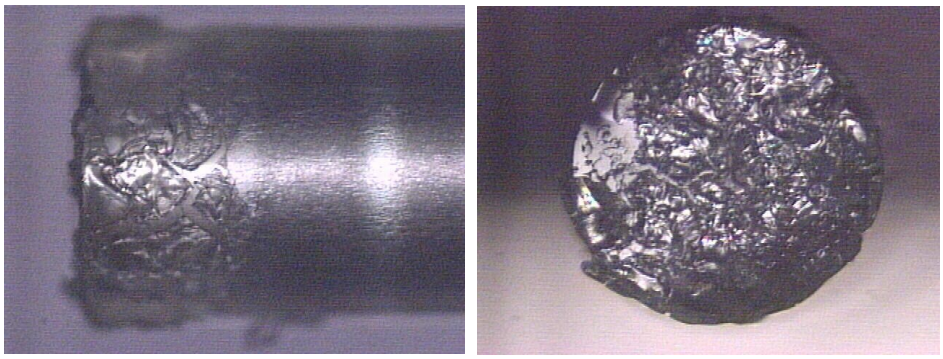

***Figure 7*:** Typical results for multilayer deposition of sol-gel solution by spray coating showing obvious cracking. The fiber diameter is 1000 µm.

Calculations (see **Table 1**) suggest that films on the order of 100 µm will be needed to maintain the simple optics of our fiber design. One solution to the problem of achieving a high cluster concentration while minimizing matrix shrinkage is to spray coat a "slurry" formed from a high concentration of particles dispersed in a of sol-gel solution. (**Figure 8**) Remillard et al. have demonstrated the deposition of >100 µm films of copper containing zeolites on the tips of high temperature optical fibers [6]. In this case, the particles are derived by pulverizing a previously aged and cured sol-gel matrix containing a high concentration of $K_2Mo_6Cl_{14}$ clusters. In short, the sol-gel solution acts as the glue to immobilize the pulverized particles at the end of an optical fiber or on a planar substrate. Advantages of this technique include minimization of shrinkage and by consequence cracking and speeding up the cure process. Another advantage of this approach is that it lends itself to standardization of the deposition process since the sol-gel solution and cluster-containing particles can be prepared separately, leading to less sample to sample variation and improved reliability.

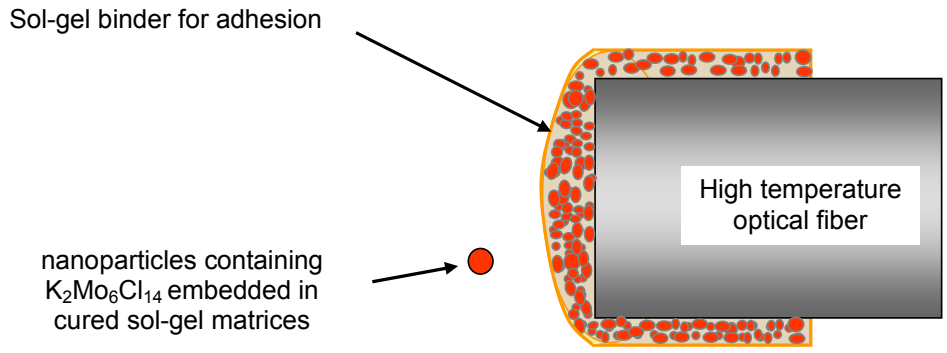

***Figure 8*:** Schematic shows the expected morphology resulting from spray deposition of slurry of particles a sol-gel solution. The particles correspond to pre-cured sol-gel particles containing $K_2Mo_6Cl_{14}$ clusters.

We have purchased two different UV transparent fibers for fabrication of the high temperature sensors which are shown in Table 1. The Ceramoptec and Fiber Guide products are rated for continuous operation at 400 and 200 °C respectively. The upper temperature limit of UV transparent fiber is primarily determined by the jacket material. Polyimide has a higher temperature rating than Tefzel (Dupont Teflon), however polyimide jacketed fibers are commercially available only with smaller core diameters than Tefzel. A large diameter fiber allows us to maximize the number of clusters on the fiber tip. In order to maximize the collection of the fluorescence signal from the lumophores immobilized at the tip of the fiber sensor, we want a fiber with a large numerical aperture (NA). The NA is a measure of the acceptance cone of light into the fiber and is proportional to the difference in index of refraction between the core and cladding (see ***Figure 9***). Both the Ceramoptec and Fiber Guide products have Fl doped claddings, which limits the NA to 0.22. Note that although the 3M fiber has a Tefzel jacket, its operation temperature is limited to 125 °C due to the use of a flouro-polymer acrylate (TECS) cladding. The advantage of the TECS cladding is that one can achieve large index steps with commensurate large numerical apertures. Following detailed discussions with several fiber manufacturers we determined that the Ceramoptec and Fiber Guide products are our optimum choices.

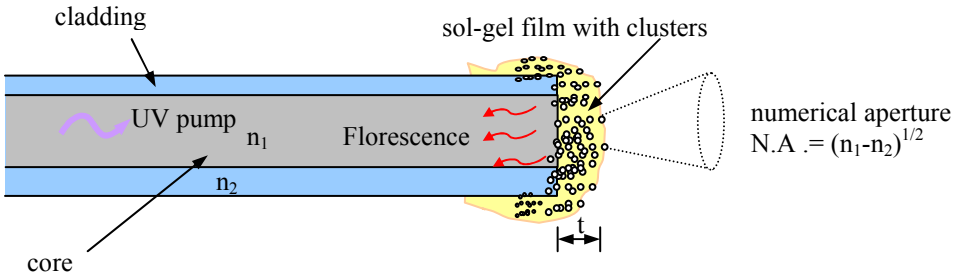

Figure 9: Reflection mode fiber optic oxygen sensor. The luminescent clusters are immobilized at the far end of the optical fiber in a sol-gel matrix. Upon UV irradiation the clusters isotropically emit red fluorescent photons. The number of fluorescent photons reflected back into the fiber is a function of the number of cluster in the film of thickness t and the numerical aperture (NA) or collection angle of the fiber.

In Table 1 we show the calculated sensor signal strength for the two high temperature fibers relative to our previous room temperature results [5]. In the room temperature case, for a 100 µm thick polymer/cluster composite we obtained a signal of 1.0 nW in a 21% O_2 environment and a signal of 7.5 nW in pure N_2 [5]. One nW of signal at the peak emission wavelength of 750 nm corresponds to 7 x 10^9 photons/s. According to our calculations at 200 °C we expect from the Ceramoptec fiber a signal of 6 x 10^8 photons/s, which should give as plenty of signal to noise as the dark counts on a typical photomultiplier or Si diode detector is ~1000.

Fiber	Core diameter (µm)	NA	Operating temp. (°C)	Relative sensor signal* (calculated)	Jacket diameter (µm)	Cladding diameter (µm)	Source Part number
1	600	0.22	400	0.088	Polyimide 710	660	Ceramoptec UV600/660P
2	1000	0.22	200	0.25	Tefzel 1850	1100	Fiber Guide SFS1000/1100Z
3	1500	0.39	125	1.0	Tefzel 2000	1550	3M FT-1.5-UMT
*Assuming a 100 µm thick sol-gel/cluster composite on the tip of the fiber with 2.9 x 10^{19} clusters/cm^3							

***Table I*:** Calculated performance of two different high temperature fiber sensors (1, 2) as compared to our previous room temperature (3) sensor. In the room temperature case for a 100 µm thick polymer/cluster (Mo_6Cl_{12}) composite we obtained a signal of 1.0 and 7.5 nW in 21% O_2 and pure N_2 respectively [5].

The performance of the Ceramoptec and Fiber Guide fibers were calculated based on our previous room temperature sensor and assuming:

(i) all the clusters in the film of thickness t emit fluorescent photons into 4π steradians
(ii) of these photons the fraction NA/4π are collected by the fiber
(iii) the quantum yield of $K_2Mo_6Cl_{14}$ is the same as Mo_6Cl_{12}. Note that similar quantum yields have been obtained for the neutral Mo cluster and butyl-ammonia salts in acetonitrile [9]
(iv) the pumping efficiency of our new setup (**Figure 16**) is the same as in [5]
(v) the collection efficiency of our new setup (**Figure 16**) is the same as in [5]

High temperature survivability of $K_2Mo_6Cl_{14}$/sol-gel films.

We measured the optical properties of sol-gel films embedded with $K_2Mo_6Cl_{14}$ after they were subjected to heating protocols where both temperature and time were varied. We used the measured luminescence intensity of the film in nitrogen and its quenching in air as an indication of the high temperature survivability of each film. A series of potassium-salt/sol-gel film slides (29-34) were prepared and then subjected to a variety of thermal processing schedules (see details in **Figure 1**). The properties of three samples, 29L, 29K, and 33H, are described in detail in this report. Film 29L is representative of the majority of coated slides prepared to date; it was cured for 24 hours at 70°C. Slide 29K has a high luminescence and was processed similar to 29L, while 33H incorporated two changes in our processing scheme, high temperature curing and the addition of A200

fumed silica in an attempt to minimize densification of the sol-gel film at high temperature, which decreases the porosity and quenching.

The emission spectra in nitrogen of film 29L and an acetonitrile solution of the potassium salt (FJ-17) used in the preparation of the film are shown in **Figure 10**. Film 29L was dip coated three times using a 9-day old Mo-cluster/sol-gel solution, dried for 21 days under ambient conditions, and then cured for 24 hours at 70°C. The film was then aged in air at room temperature for 3 months. Using a variety of time and temperature combinations, film 29L was annealed at 200°C for a total of 54 hours, with the emission spectra measured after each heating step. After subtracting the Raman scattering due to the sol-gel matrix we found that the line-shape had not changed, confirming that sol-gel immobilization and thermal cycling did not adversely affect the emission of the potassium salt (FJ-17).

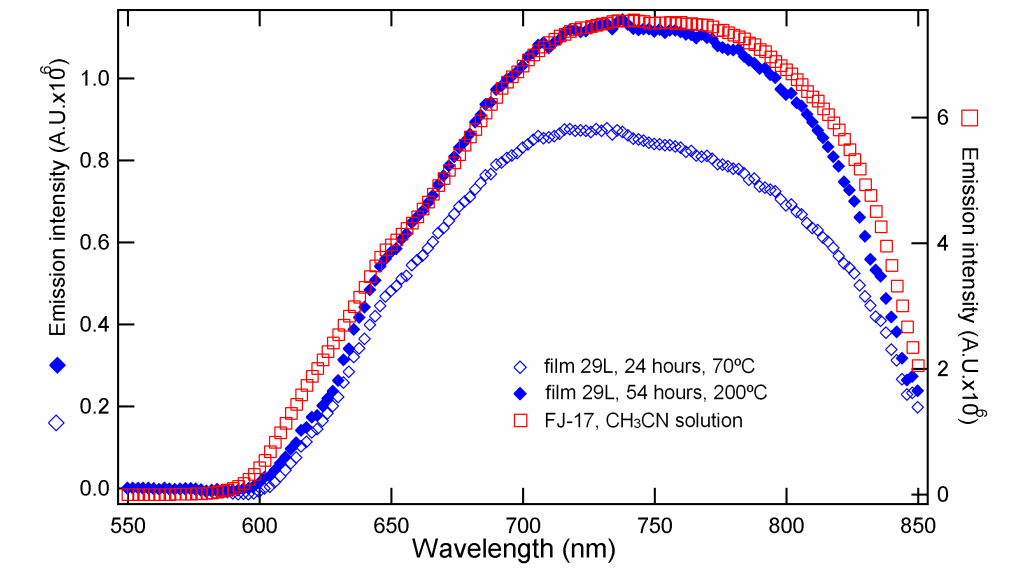

***Figure10*:** Room temperature emission spectra sol-gel film 29L (◇) 1 day curing at 70°C, (◆) 54 hours of thermal cycling between 200 °C, and the spectrum of its originating potassium salt FJ-17 (□) in CH_3CN. All spectra were measured and in 99.999% nitrogen. The film concentration is 3.6 ± 1.6 x10^{21} cluster/cm^3 based on an estimated film thickness of 700 ± 300 nm. The solution concentration is 0.087 mM ± 1.4%.

Shown in **Figure 11** is the emission intensity of 29L measured in nitrogen after each thermal cycle at 200 °C. The data have been corrected for variations in the lamp intensity. Note that the luminescence intensity is nearly constant over the entire time interval, demonstrating the long-term stability of the cluster photophysics, even after extended aging at 200°C. However, we observed that the oxygen quenching ratio, defined as the ratio of the luminescence intensity in 99.999% N_2 to that in 21% O_2, decreased to 1.2 at the conclusion of the tests.

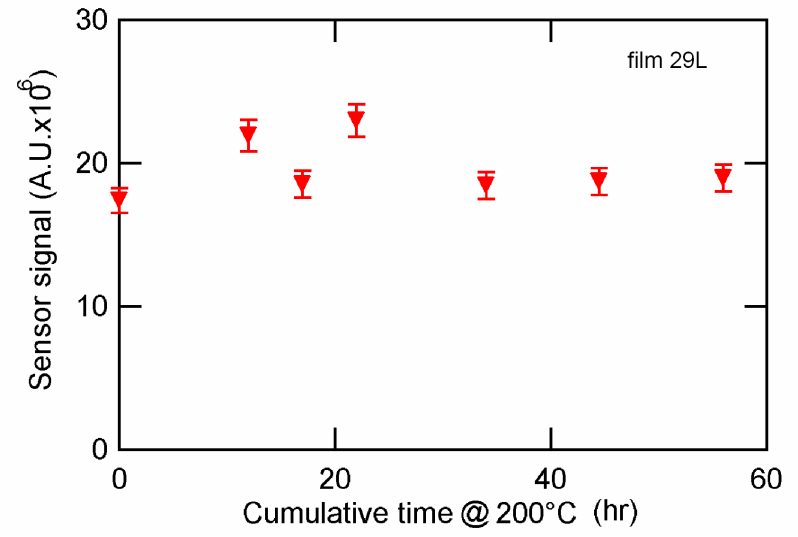

***Figure 11*:** Integrated emission intensity (550 - 850 nm) from sol-gel film 29L at room temperature, after heating at 200°C for the indicated time interval. See Figure 10 for cluster information.

Sol-gel matrix effects on quenching

A critical design issue is the matrix used to embed the lumophores. It must have a high oxygen permeability to achieve near real-time oxygen sensing and a high quenching ratio. We attribute the decrease of the quenching ratio for 29L to densification of the sol-gel matrix which reduces the permeability of the film. Real time data for oxygen quenching are shown in **Figure 12**. Annealing at 200 °C increases the time needed to reach equilibrium as well as decreasing the quenching ratio. Before annealing, 29L quenched by 3× in ~15 seconds, compared to 1.2× in `15 minutes after annealing. Since the luminescence intensity itself remains approximately constant, the slow quenching must correspond to decreased permeability of oxygen through a densified sol-gel matrix. We tested different curing conditions in an attempt to improve quenching in annealed sol-gel films. Preliminary results using a fast curing protocol, 0.5 hr at 200 °C looked promising, but the quenching ratios for these films also declined after annealing.

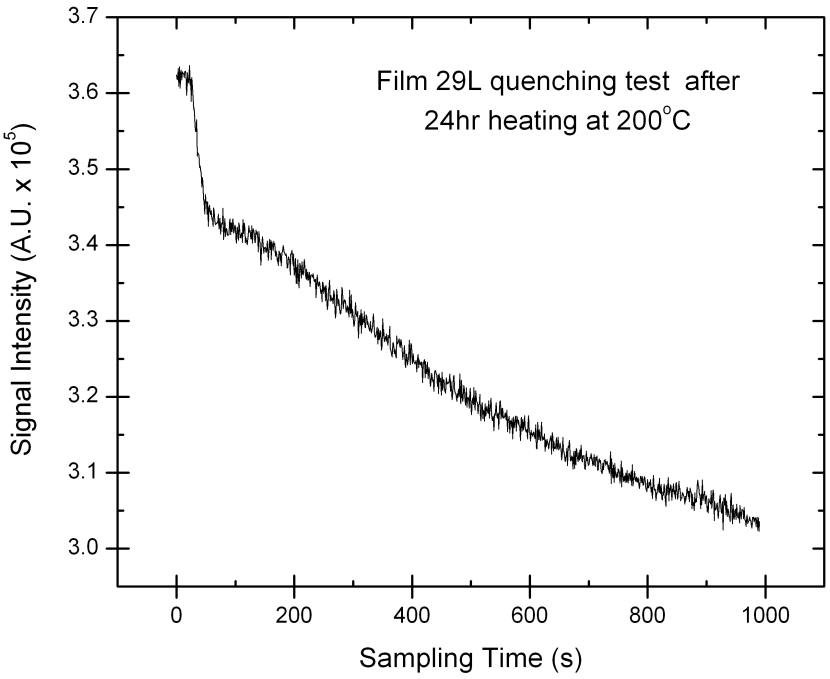

***Figure 12*:** Response of film 29L after 24 hours of heating at 200°C to a step change in gas from 100 N_2 to 21% O_2 at 75 s. The quenching ratio remains at 1.2×, but the quenching time increases to >15 minutes. Densification of the sol-gel matrix after thermal processing leads to a low oxygen permeability.

As noted in our previous report, the permeability of sol-gel matrices is related to the free volume within the matrix and is highly dependent on the details of the synthetic parameters used to prepare the sol-gel matrix cell gel. Briefly, a sol-gel synthesis involves the acid or base catalyzed hydrolysis and condensation of metal alkoxides such as tetraethylorthosilicate (TEOS). As the reaction proceeds to completion the sol-gel solution is converted to a continuous solid matrix. If spectator compounds are present, in our case $K_2Mo_6Cl_{14}$, they are entrapped within the matrix. Essentially all sol-gel films densify to some extent as they cure and further densify after drying at high temperatures. However, the porosity of the final matrix can be potentially altered by the addition of a diluent or A200 fumed silica by adjusting the processing conditions used to cure and dry the matrix. For example, added solvent reduces the concentration of TEOS and favors the formation of individual silica particles in the sol-gel solution. Films cast from such a solution will tend to be locally heterogeneous and have a high free volume. In contrast, casting a sol-gel solution before substantial particle formation has taken place leads to a more uniform film, but with a higher density and lower permeability. Using this approach, we prepared several slides where A200, a nanoparticulate fumed silica was included in the sol-gel solution. The initially cured filmed showed good permeability, but densification on annealing remains a problem.

***In-situ* spectroscopy**

Another concern is the intrinsic temperature dependence of the luminescence intensity of $K_2Mo_6Cl_{14}$ sol-gel films. **Figure 13** shows real-time measurements of the luminescence intensity in switching between 100% N_2 and 21% O_2 as a function of temperature. We observed quenching at temperatures >200 °C. At lower temperatures, the luminescence intensity is large with a quenching ratio of 1.55×. Although the intensity decreases with temperature, the quenching ratio remains approximately constant. At the highest temperature, 215 °C, the intensity drop is 10dB compare to room temperature, but the quenching ratio is 1.3×. The change in the luminescence is completely reversible, leading us to believe that the effects do not correspond to permanent photobleaching typically seen with organic lumophores. Further experiments are needed to elucidate the mechanism responsible for the temperature dependence of the luminescence intensity.

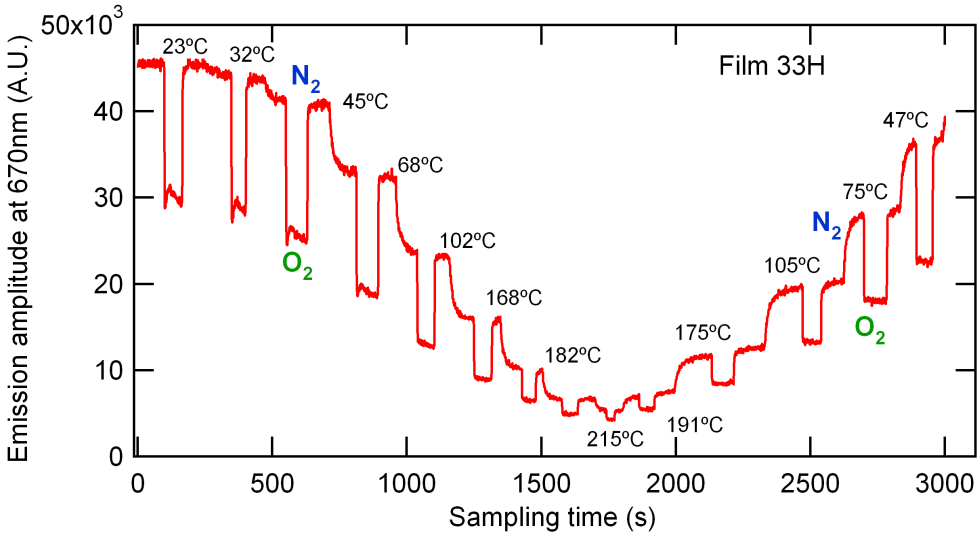

***Figure 13*:** Real-time luminescence intensity at 670 nm for sol-gel film 33H (MM5 + A200 fumed silica) during gas exchange from 100% N_2 to 21% O_2. These *in-situ* emission measurements were made at the indicated temperatures using a Pt microheater attached to the back of the slide. At each temperature, data were collected for 60 -120 s, during which time the emission intensity reaches ~90% of the steady state value. The lumophore concentration is approximately $(2.12 \pm 0.5)\times10^{22}$ clusters/cm^3 using an estimated thickness of 700 ± 200nm.

Figure 14 shows the in the integrated emission intensity in N_2 and O_2 as a function of temperature for film 29K. The quenching ratio varies between 1.4 to 1.9 between room temperature and 210 °C. The data is approximately linear on a logarithmic scale indicating that the emission intensity varies exponentially with temperature. Upon returning to room temperature the luminescence intensity returned to close to its original value. The detector dark noise is <10% of the signal at 200°C, demonstrating that there is sufficient signal/noise ratio for high temperature sensing.

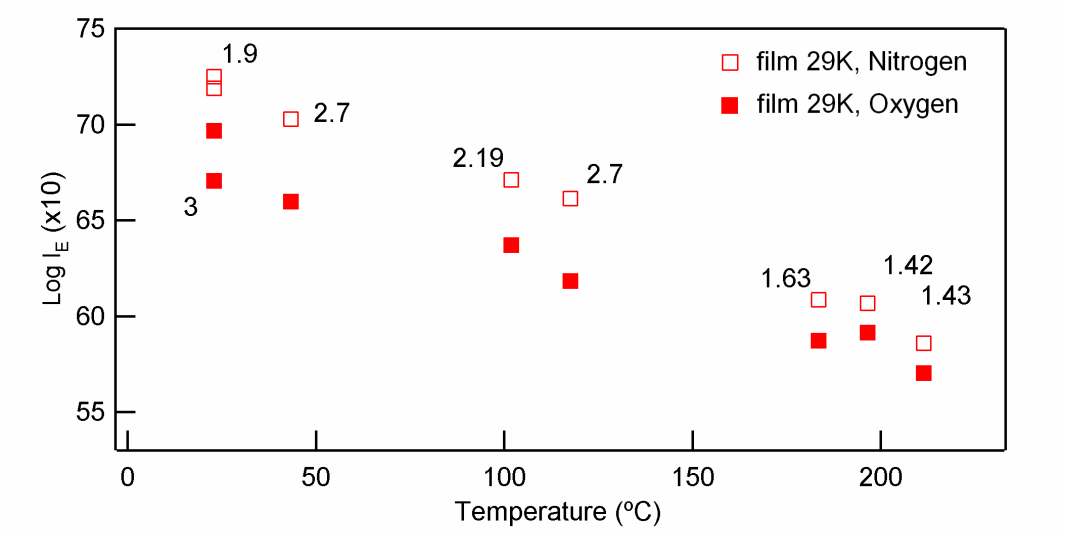

***Figure 14*:** The integrated signal intensity from i*n-situ* measurements of sol-gel film 29K (FJ-17) in (□) 99.999% N_2 and (■) 21% O_2 show an approximately exponential dependence on temperature. The logarithm of the integrated emission intensity (I_E) is plotted on the y-axis. The quenching ratio at each temperature is indicated; these values demonstrate the long-term stability of the clusters at high temperature. The film concentration is 3.6 ± 1.6 x10^{21} cluster/cm^3 based on an estimated film thickness of 700 ± 300 nm.

There are two physical mechanisms that could give rise to the observed temperature dependence of the luminescence intensity. The first is an intrinsic temperature dependence of the cluster photophysics. In other words, temperature dependence of the population of the excited electronic state responsible for the red luminescence (which affects the number of luminescent clusters) or temperature dependence of the excited to ground state transition rate. Azumi and Saito [10] have measured the temperature dependence of the phosphorescence lifetime (τ) of crystalline $[(C_2H_5)_4N]_2$ $[Mo_6Cl_{14}]$ from 4.2 K to room temperature, and observe a linear decrease in τ from 130K to 273K. Extrapolation of these measurements to higher temperature is not consistent with the exponential decrease in luminescence that we observe. The second possibility is a temperature dependent cluster sol-gel matrix interaction which results in fewer optically "available" clusters at higher temperature. In light of Azumi's data we postulate that the second mechanism is more likely than the first. In either case a higher cluster concentration in the film, would ameliorate the signal to noise problems of the fiber sensor at 200 °C due to a reduction in luminescence intensity.

Fiber optic oxygen sensor characterization system

Unlike the Ru-based optical indicators commonly for fiber optic oxygen sensing, the red fluorescence from the hexanuclear molybdenum clusters can be easily measured using an intensity based scheme. This is due to the large Stokes shift (> 300 nm) and long cluster lifetime (>100 μs). Shown in **Figure 15a** is the system we use to rapid evaluation of $K_2Mo_6Cl_{14}$/sol-gel films on quartz slide or on a fiber in terms of the luminescence signal intensity and oxygen quenching ratio.

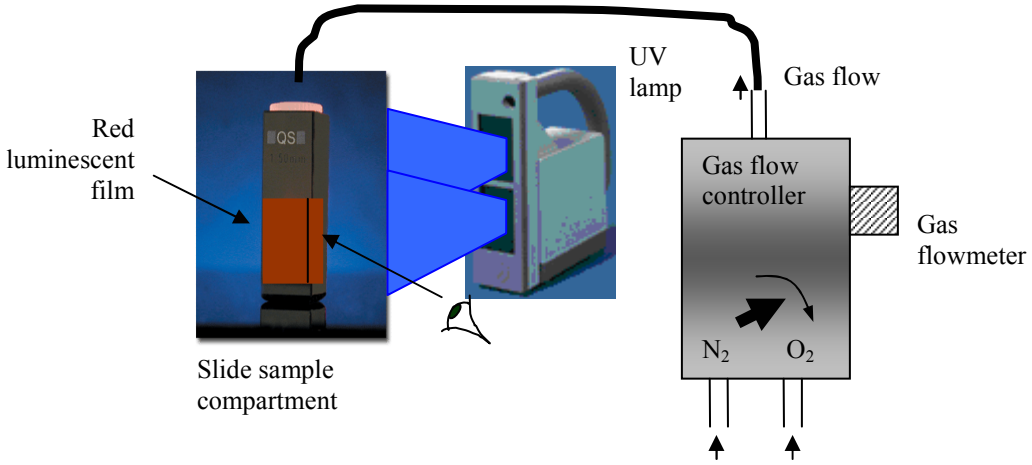

Figure 15: System for rapid evaluation of $K_2Mo_6Cl_{14}$/sol-gel films on quartz substrates. The film is placed inside a quartz cell, the gas in the cell can be rapidly changed between 21% O_2 and 100% N_2. By illuminating the sample in a dark room with a 365 nm lamp, we can observe by eye the change in the red luminescence intensity. Note that the human eye is capable of detecting single photons, after about 10 minutes of adjustment in a dark room.

We have also designed and begun building a setup for automated high temperature reflection-mode fiber optic sensor measurements (see **Figure 16**), which will be fully operational in May 2005. The ceramic "furnace" allow us to heat the tip of the fiber sensor up to ~220 °C. Using a thermocouple and computer controlled feedback system we will be able to control the temperature to better than ± 5 °C. Using typical laboratory gas flows, ~100ml/min, we estimate that the gas exchange time in the ceramic "furnace" will be <10 s, which will allow us to determine the time response of the sensor.

Our goal is to demonstrate an inexpensive and portable fiber optic sensor system. We will use a commercial 365 nm UV LED from Nichia that costs $6 for the excitation source. Note that back in 1999, our only choice was to use a $30,000 HeCd laser for excitation. We have been able to couple 0.5 mW of UV light into our high temperature fibers with the LED; which is the same excitation power we used for the room temperature sensor [5]. The sensor will operate in reflection mode, by pumping and collecting the reflected luminescence signal from the same end of the fiber. The signal and pump beams will be separated using a 45° long wave pass (LWP) dichroic beam splitter and 590 nm LWP filter. The detection optics/electronics will be composed of a Si detector (UTD) with a 0.5W/A efficiency followed by a current pre-amplifier with 10^9

V/A gain. If stray signal due to scattered light becomes a problem, we plan to modulate the UV LED at a few kHz and collect the first harmonic of the detector signal to remove scattered light from the intensity based measurement. Using a LabView interface the entire system will be computer controlled to allow for real time control and monitoring of the optics, gas flow and thermometry.

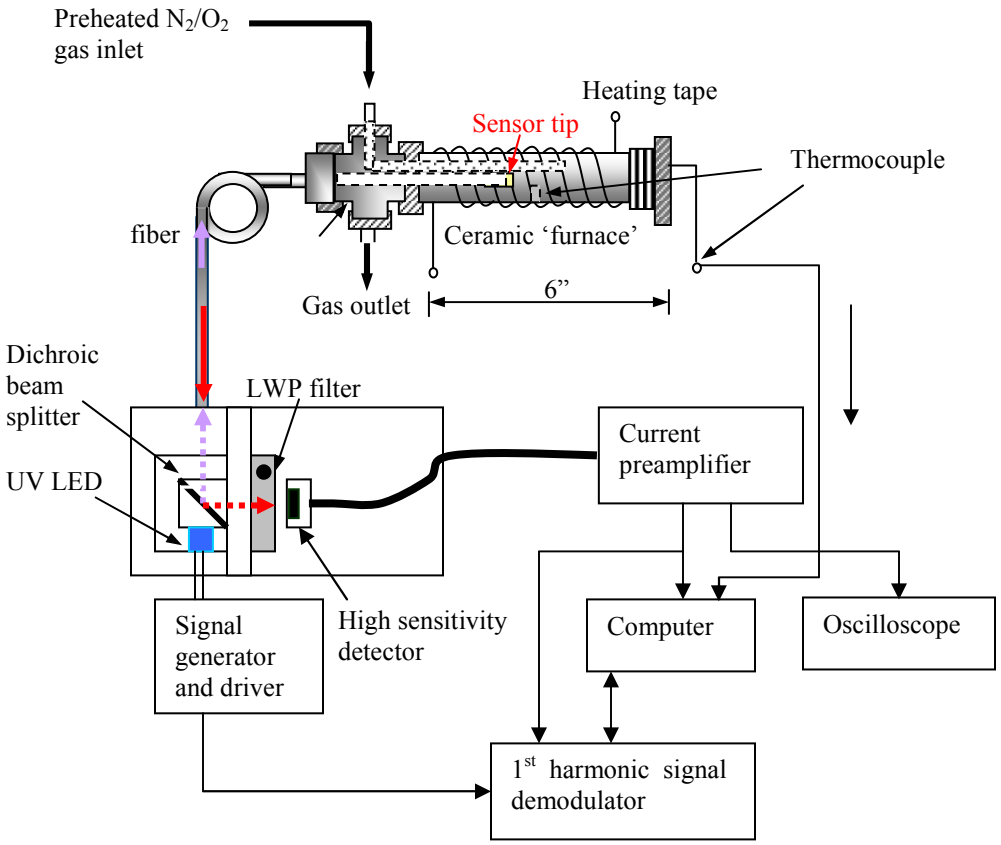

***Figure 16*:** Setup for automated high temperature reflection-mode fiber optics oxygen sensor measurements. A heated gas stream, 30 – 220 °C, impinges on the fiber sensor tip at a flow rate of ~100 ml/min. The gas exchange time in the ceramic "furnace" is <10 s. The sensor is illuminated with 365 nm light from a LED, and the reflected red luminescence from the fiber tip is collected by a high sensitivity detector (Si photodiode or a photo-multiplier tube). The excitation source, detection optics and temperature control are all computer controlled through a LabView interface.

CONCLUSIONS

TGA experiments confirm that superior thermal stability of $K_2Mo_6Cl_{14}$ compared to Mo_6Cl_{12}. They experiments also suggest that long term, continuous applications of $K_2Mo_6Cl_{14}$ are likely for temperature <250° C, with some tolerance for short-term high-temperature excursions. We also have defined the experimental parameters that lead to thermally robust $K_2Mo_6Cl_{14}$ / sol-gel films. From two independent runs we have demonstrated that quenching between 99.999% N_2 and 21% O_2 of a factor of four can be obtained following thermal cycling of half an hour at 200 °C. Experiments are underway to corroborate these results with *in-situ* measurements of the luminescence and quenching ratio as a function of temperature. In addition we are investigating the upper bound in terms of both temperature and time on the thermal stress cycle of these potassium salt / sol-gel films.

We have purchased UV transparent optical fibers, rated for continuous operation from 200 to 400 °C, for sensor fabrication. Both the quenching ratio and the number of photons available are promising for development of a $K_2Mo_6Cl_{14}$ based sensor. In addition, our calculations indicate that we have sufficient signal to noise ratio to observe the sensor signal at elevated temperature during gas exchanges between 21 % O_2 and pure N_2. A 23 – 220 °C set-up for testing fiber sensors is under construction. Our timeline for demonstrating a high temperature fiber oxygen sensor is given below.

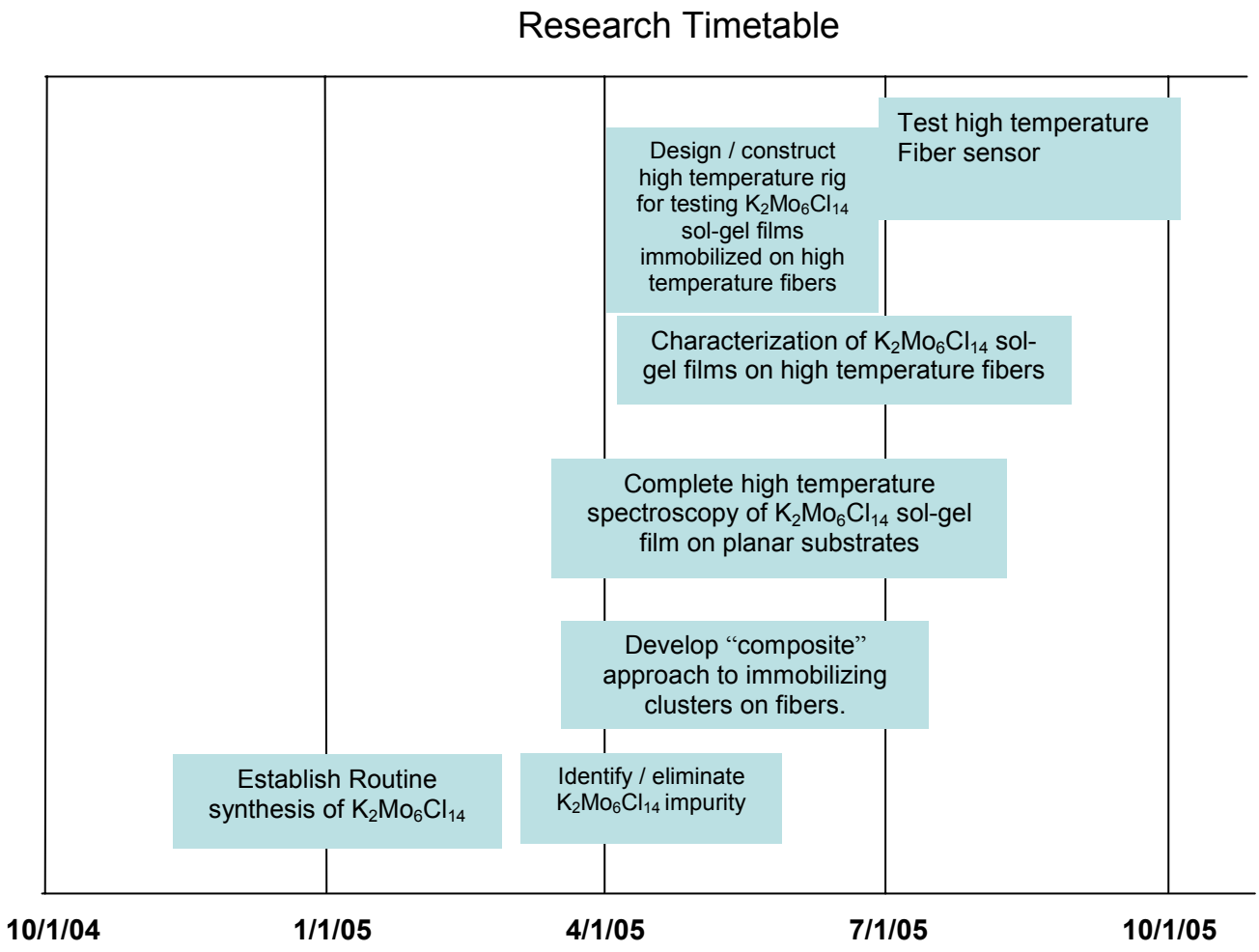

REFERENCES

[1] R. D. Mussell, Ph. D. thesis, Michigan State University (East Lansing), **1988**.
[2] M. D. Newsham, Michigan State University (East Lansing), **1988**.
[3] M. D. Newsham, M. K. Cerreta, K. A. Berglund, D. G. Nocera, *Mater. Res. Soc. Symp. Proc.* **1988**, *121*, 627.
[4] C. J. Ruud, Ph. D. thesis, Michigan State University (East Lansing), **1999**.
[5] R. N. Ghosh, G. L. Baker, C. Ruud, D. G. Nocera, *Appl. Phys. Lett.* **1999**, *75*, 2885.
[6] J. T. Remillard, J. R. Jones, B. D. Poindexter, C. K. Narula, W. H. Weber, *Appl. Opt.* **1999**, *38*, 5306.
[7] J. C. Sheldon, *J. Chem. Soc.* **1960**, 1007.
[8] L. M. Robinson, H. Lu, J. T. Hupp, D. F. Shriver, *Chemistry of Materials* **1995**, *7*, 43.
[9] A. W. Maverick, J. S. Najdzionek, D. MacKenzie, D. G. Nocera and H. B. Gray, *J. Am. Chem. Soc*., **1983**, *105*, 1878.
[10] T. Azumi and Y Saito, *J. Phys. Chem.*, **1988**, *92*, 1715.

BIBLIOGRAPHY

None.

LIST OF ACRONYMS AND ABBREVIATIONS

HCl – Hydrochloric Acid
MeOH – Methanol
CH_3CN – Acetonitrile
TEOS – Tetraethyl orthosilicate

APPENDIX A - ACKNOWLEDGEMENTS

We wish to acknowledge the contribution of Reza Loloee, Michigan State University, towards the gas flow switch box and calculation of high temperature gas flow rate.